

EFFECT OF SOIL NON-LINEARITY ON THE SEISMIC RESPONSE OF A VERY SOFT ALLUVIAL VALLEY

Fani GELAGOTI¹, Rallis KOURKOULIS², Ioannis ANASTASOPOULOS³, George GAZETAS⁴

ABSTRACT

To develop insight into the sensitivity of 2D wave effects to soil non-linearity, a numerical study is conducted, utilizing a shallow soft valley in Japan (the Ohba Valley) as a test case. Overall, soil nonlinearity may modify the 2D valley response to a substantial extent. The Aggravation Factor (AG) at the center of the valley is significantly reduced with increasing soil nonlinearity while, quite remarkably, AG at the valley edges may increase due to the trapping of multi-refracted waves into a narrow plastified zone. The analyses revealed the generation of a quite important parasitic vertical acceleration component close to valley edges. The latter, being a direct result of 2D wave refractions, is well correlated and of similar frequency content with the horizontal component and could therefore be very detrimental to structures.

Keywords: 2-D wave effects, valley, amplification, non-linear constitutive model

INTRODUCTION

Although the dynamic response of valley formations has been extensively investigated in the literature, research interest has mainly concentrated on sine-shaped, cylindrical, and trapezoidal valleys subjected either to harmonic excitations or to single pulses. Assuming elastic soil response, numerous closed form expressions have been derived to quantify the 2-D amplification phenomena (Trifunac, 1971, 1973; Bouchon; 1973; Kawase; 1987; Sanchez-Sesma & Rosenbluth, 1979; Fishman & Ahmad, 1995). Of particular interest is the work of Bard & Bouchon, 1980. Utilizing the theoretical Aki-Larner technique (AL) they studied the dynamic response of two different valley formations due to incident SH, SV and P waves: a cosine shaped valley and a flat bottom valley bounded by steep edges. Among various valuable findings, they concluded that surface waves generated at the valley boundaries (Love waves, when the excitation is SH waves; Rayleigh waves in case of SV and P waves) propagate back and forth resulting in significant amplifications along the valley surface. Similar were the findings of Harmsen & Harding (1981), and Othuki & Harumi (1983). Some years later Bielak and his coworkers presented a comprehensive study on the effect of 3D valley geometry on the produced amplification (Bao et al., 1996; Bielak et al., 1999; 2000). One of the first attempts to account for soil-nonlinearity when studying wave propagation problems was that of Zhang & Papageorgiou (1996). They numerically simulated the non-linear response of the Marina District during the Loma Prieta earthquake and highlighted the detrimental effect of soil inelastic response on wave focusing effects.

This paper further extends the work presented by Gelagoti et al, 2007 (where the sensitivity of 2D wave effects to the frequency content and the “details” of the input motion were examined) and focuses on how

¹ Doctoral Researcher, Soil Mechanics Laboratory, NTUA, e-mail: fanigelagoti@gmail.com

² Post Doctoral Researcher, Soil Mechanics Laboratory, NTUA.

³ Post Doctoral Researcher, Soil Mechanics Laboratory, NTUA.

⁴ Professor, School of Civil Engineering, NTUA.

and to what extent the soil induced non-linearity may modify the seismic response of a very soft alluvial valley. Emphasis is given on the generation of parasitic vertical component, the effects of which may be detrimental for overlying structures, a phenomenon which has so far received scarce attention.

PROBLEM DEFINITION AND ANALYSIS METHODOLOGY

Problem Definition

Situated close to Fujisawa City in Japan, the Ohba Valley is as an extremely-soft alluvial basin. The geometry of the valley and the soil profile are shown in Fig. 1(a) (adapted from Tazoh et al., 1984). At the top layers (20 to 25 meters) the N_{SPT} values of the standard penetration test are very close to zero, while the shear wave velocity, V_s , measured through down-hole tests, ranges between 40 and 65 m/s. The underlying substratum consists of Pleistocene diluvial deposits with N_{SPT} values greater than 50 and V_s around 400 m/s. The ground water table is almost at the ground surface, while the water content of the top layers by far exceeds 100 %.

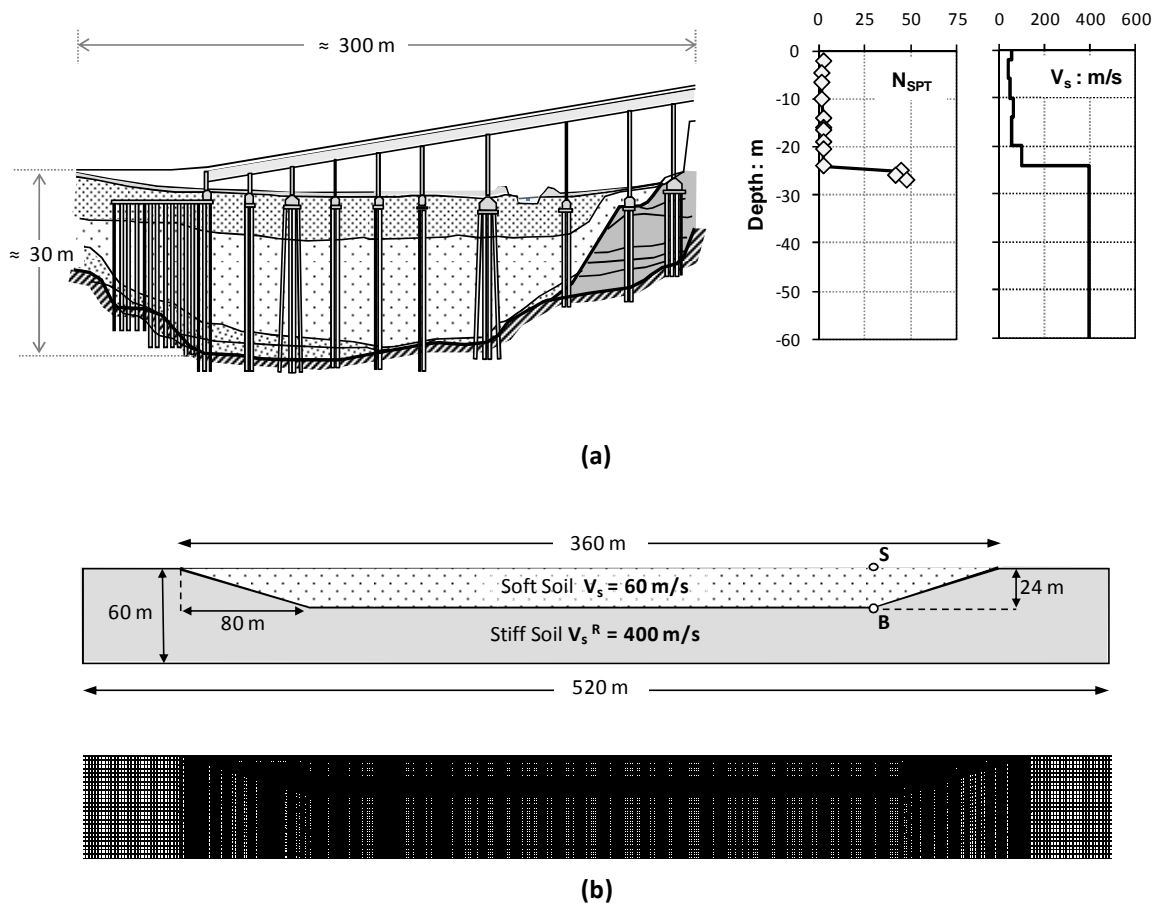


Figure 1: (a) Cross section of the Ohba Valley and in-situ soil properties (after Tazoh et al, 1984), (b) Idealized cross-section of the Ohba Valley and finite element discretization.

The seismic response of the valley is analyzed in the time domain employing the finite element (FE) method, assuming plane-strain conditions. The idealized geometry of the valley and the associated configuration of the FE model are depicted in Fig. 1(b). The soil is modeled with quadrilateral continuum

elements, with a very fine discretization to ensure realistic representation of the propagating wavelengths. The valley deposit is assumed homogeneous with $V_S = 60$ m/s, while the shear velocity of the substratum is significantly higher : $V_S = 400$ m/s. With mass densities of 1.4 and 1.9 Mg/m³, respectively, the impedance contrast between soil and base, $\rho_z, v_{sz}/\rho, V_{s1}$ is about 10.). Reflections at the base of the formation are avoided by utilizing absorbing boundaries. "Free-field" boundaries responding as shear beams are placed at each lateral boundary of the model, to reproduce free- field conditions.

Two different types of analysis have been conducted : (i) visco-elastic analysis, and (ii) full nonlinear analysis utilizing the finite element code ABAQUS [2008] employing a kinematic hardening constitutive model.

Soil Constitutive Modeling

For the nonlinear analyses, a nonlinear kinematic hardening constitutive model is employed. The evolution law of the model consists of two components: a nonlinear kinematic hardening component, which describes the translation of the yield surface in the stress space (defined through the "backstress" α , a parameter which defines the kinematic evolution of the yield surface in the stress space), and an isotropic hardening component, which describes the change of the equivalent stress defining the size of the yield surface σ_o as a function of plastic deformation.

The model incorporates a Von Mises failure criterion, considered adequate to simulate the undrained response of clayey materials, with an associative plastic flow rule. The evolution of stresses is described by the relation :

$$\sigma = \sigma_o + \alpha \quad (1)$$

The evolution of the kinematic component of the yield stress is described as follows :

$$\dot{\alpha} = C \frac{1}{\sigma_o} (\sigma - \alpha) \dot{\epsilon}^{pl} - \gamma \alpha \dot{\epsilon}^{pl} \quad (2)$$

where C the initial kinematic hardening modulus ($C = \sigma_y/\epsilon_y = E$) and γ a parameter that determines the rate of kinematic hardening decrease with increasing plastic deformation (Fig. 2a).

Model parameters are calibrated against $G-\gamma$ curves of the literature, as described in Anastasopoulos et al. (2010). Figure 2(b) illustrates the results of one such calibration (through finite element simulation of the simple shear test) against the $G-\gamma$ curves of Ishibashi and Zhang (1993).

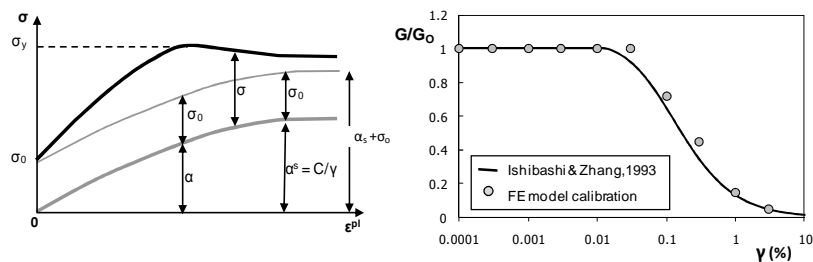


Figure 2: Parameters incorporated into the formulation of the kinematic hardening soil model used in the nonlinear analyses (left figure) and example result of the calibration procedure against published $G - \gamma$ curves from the literature (right figure).

This section compares the results of a visco-elastic analysis (assuming damping ratio of $\xi = 2\%$) with that of a fully nonlinear analysis employing the kinematic hardening constitutive model described previously. The $G-\gamma$ curves of Ishibashi & Zhang [1993] for $PI = 50$ have been utilized for the calibration of constitutive model parameters. Initially the valley is subjected only to Ricker wavelets of different frequency content with peak acceleration of $0.2g$ corresponding to moderate ground shaking (Figure 3) and the comparison is performed in terms of distribution of Aggravation Factor [AG] along the valley surface. The latter (Figure 4) is defined as the ratio of maximum calculated acceleration on the valley surface over the maximum acceleration of an 1-d analysis of the same soil profile. The following conclusions may be drawn:

For all frequencies examined soil non-linearity has resulted to a reduction of the aggravation practically along the whole length of the valley surface (the response approaches that of a 1-D formation close to the valley center as evidenced by the AG value tending to unity). The effect of soil non-linearity has been observed to be lower in case of high frequency excitation (Fig. 4a). Quite interestingly, and contrary to what would have been expected, it appears that soil nonlinearity does not always reduce AG, especially as we move towards the valley edges. The phenomenon is quite luminous in case of longer-period excitations (Fig 4(b) and 4(c)). A possible explanation is that the initially arriving incoming waves create a narrow plastified zone that subsequently acts like a "trap" for forthcoming waves. The latter keep refracting within the narrow band between the plastic zone and the surface, thus generating larger AG. This assumption will be further supported in the ensuing when the valley will be subjected to recorded accelerograms.

Three records with completely different characteristics have been employed: (a) a relatively high frequency, short duration accelerogram (Kede record, Athens 1999), a multi cycle and of higher periods record (Lefkada 2003, Greece 2003) and a high period near fault excitation (Yarimca Record, Turkey 1999). Figure 5 presents the three time histories along with their respective elastic response spectra. The comparison of the elastic with the nonlinear analysis is shown in Figure 6 again in terms of spatial distribution of AG values. The same results as the ones discussed previously hold also true for the case of real accelerograms. The least effect of soil non linearity is indeed produced by the "high-frequency" Kede (Athens 1999) seismic excitation (Fig. 6(a)). A quite remarkable concentration of high AG values is observed close to the valley edges; a direct confirmation of the effect of multiple refractions of trapped waves within the plastified soil wedge. This effect is as expected conspicuous for the Lefkada 2003 and the Yarimca seismic excitations which contain several strong motion cycles. Indeed, for the Yarimca excitation, the AG factor increases to 1.65 when soil non-linearity is considered compared to 0.80 (de-amplification) in the elastic case.

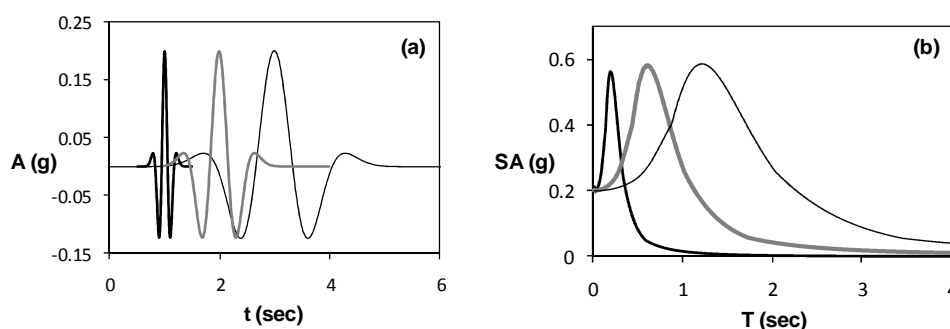


Figure 3: (a) Acceleration time history of the three Ricker wavelets used in the numerical analysis (Ricker3-thick black line; Ricker1-grey line; Ricker0.5-black line) and (b) the corresponding 5 % damped acceleration elastic response spectra.

GENERATION OF PARASITIC VERTICAL COMPONENT

In the previous sections, the aggravation due to 2-D valley effects has been investigated, focusing to the prevailing horizontal component of the seismic motion. However, due to the geometry of the bedrock slope, a purely horizontal seismic motion will unavoidably generate a parasitic vertical component. In the sequel, a first attempt to address such phenomena is attempted. The results presented in the ensuing refer to the valley being subjected to real earthquake excitations, while both elastic and non-linear soil has been considered. Figure 7(a) presents the spatial distribution of the ratio of the valley-generated parasitic vertical component A_v to the horizontal component A_h ($\max A_v / \max A_h$) when the valley is subjected to the horizontal component *only* of the Kede record (Fig. 5(a)) and assuming elastic soil response. Interestingly, as revealed by the distribution of the $\max A_v / \max A_h$ ratio (Fig. 7(a)), as we move towards the valley edges, a strong vertical motion is observed. Yet this parasitically generated vertical component A_v may be equal or even greater than the corresponding horizontal A_h motion. On the other hand, being mainly the result of geometry (or "focusing") effects, this parasitic vertical component almost disappears at the center of the valley. Figure 7b compares the time histories of the valley-affected horizontal acceleration with that of the parasitically generated. Note that since the valley-generated A_v is the result of geometry, the two motions are totally correlated in time domain, while they have very similar frequency content (as expressed by the elastic response spectrum) with the vertical motion to appear slightly more high frequency. For the "intermediate" Lefkada 2003 (Fig. 8) and the "low-frequency" Yarımcı (Fig. 9) the key conclusion remains. However the observed $\max A_v / \max A_h$ ratio is quite lower (it never exceeds the value of 0.65).

Finally, Figure 10 highlights the effect of soil inelastic response to the amount of vertical motion experienced at the valley surface. It is clear that the amplitude of the parasitic vertical component (compared to the amplitude of the corresponding horizontal component) is slightly decreased by with induced soil nonlinearity. This decrease is almost invisible for the "high-frequency" Kede seismic excitation (Fig. 10a), and becomes more evident for the "intermediate" Lefkada 2003 (Fig. 10b) and the "low-frequency" Yarımcı case (Fig. 10c)

CONCLUSIONS

A numerical study has been conducted to highlight the role of soil nonlinearity on the seismic response of a very soft alluvial valley. The following conclusions have emerged :

- 1) Soil nonlinearity may modify the 2-D valley response to a substantial extent. For idealized single-pulse (Ricker) seismic excitations, soil nonlinearity in general reduces AG, mainly at the center of the valley (where the role of surface waves is dominant). Under real seismic excitations the general trends are preserved though somehow more complicated: Soil plastification near the soil-rock interface at valley edges, leads to the development of a very soft plastified zone. Particularly when the excitation contains a large number of strong motion cycles, this plastified zone may act as a "trap" for incident waves and hence may result in intensified focusing phenomena as denoted by the large AG values towards the valley boundaries.
- 2) The 2-D geometry of the valley (excited by exclusively-horizontal waves) generates a "parasitic" vertical component. In contrast to the natural vertical component of an earthquake, which is the result of P-waves and is usually of very high frequency content to pose a serious threat to structures, this valley-generated parasitic vertical component *may be detrimental for overlying structures* : being a direct result of geometry, it is fully correlated and of practically the same dominant period as the horizontal component.

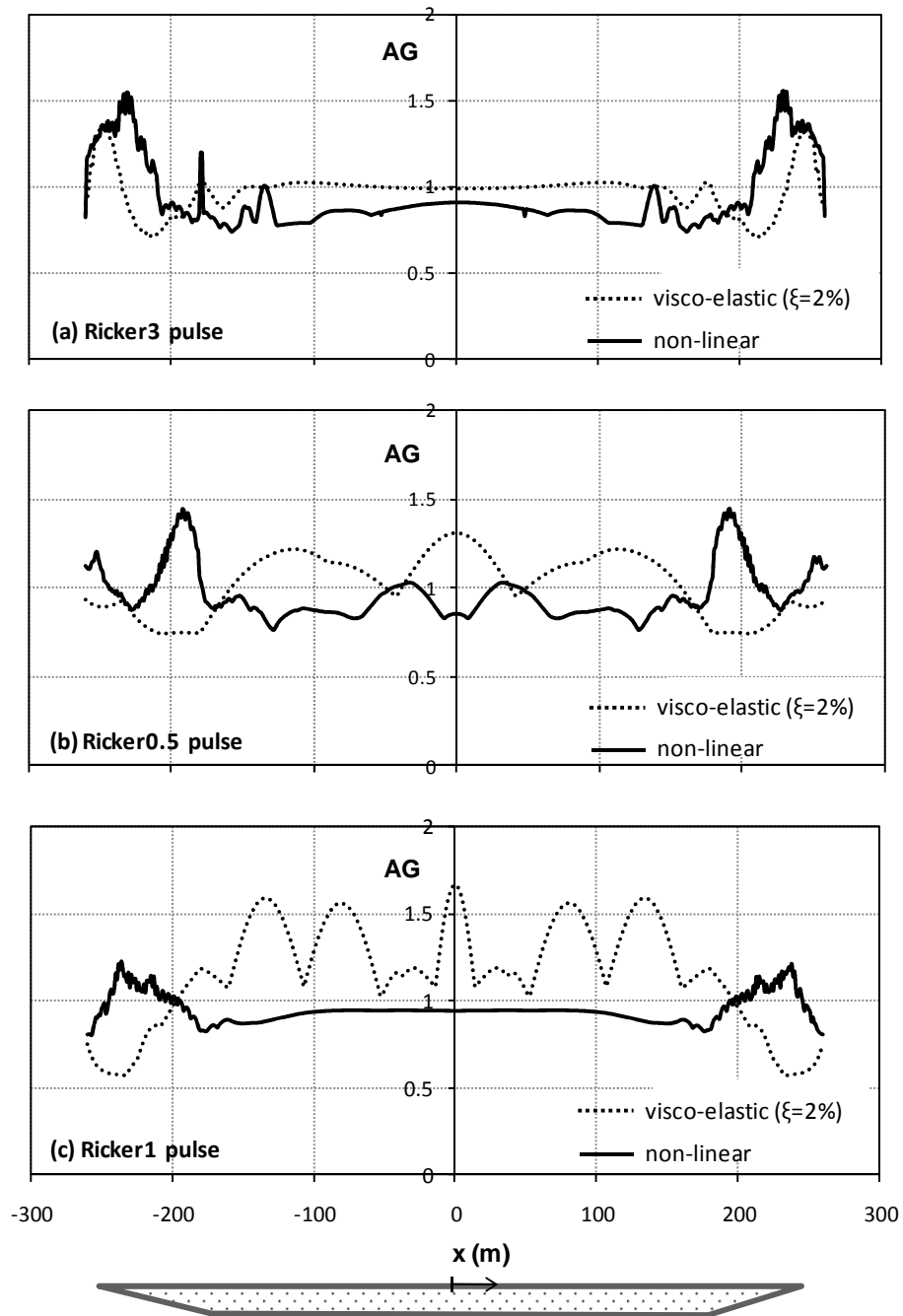


Figure 4: Elastic vs Non-linear Response comparison in terms of aggravation factor when the valley is subjected to: (a) the Ricker3, (b) the The Ricker0.5 wavelet and (c) the Ricker 1 wavelet, all scaled at 0.2 g

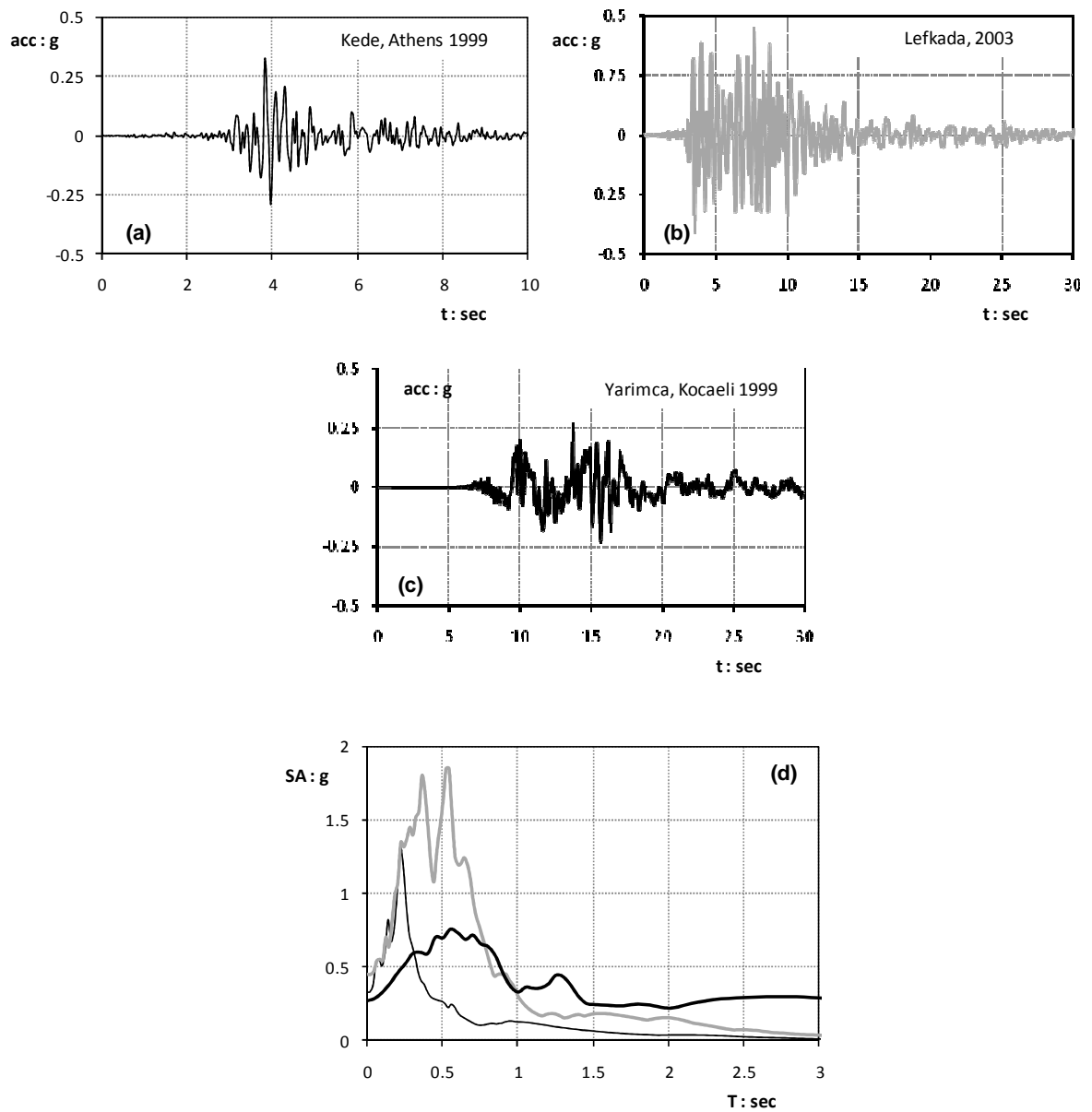


Figure 5: Acceleration time histories of the three earthquakes used in the numerical analyses : (a) Kede record (Athens,1999), (b) Lefkada 2003, (c) Yarimca record (Turkey 1999) and (d) comparison of elastic response spectra

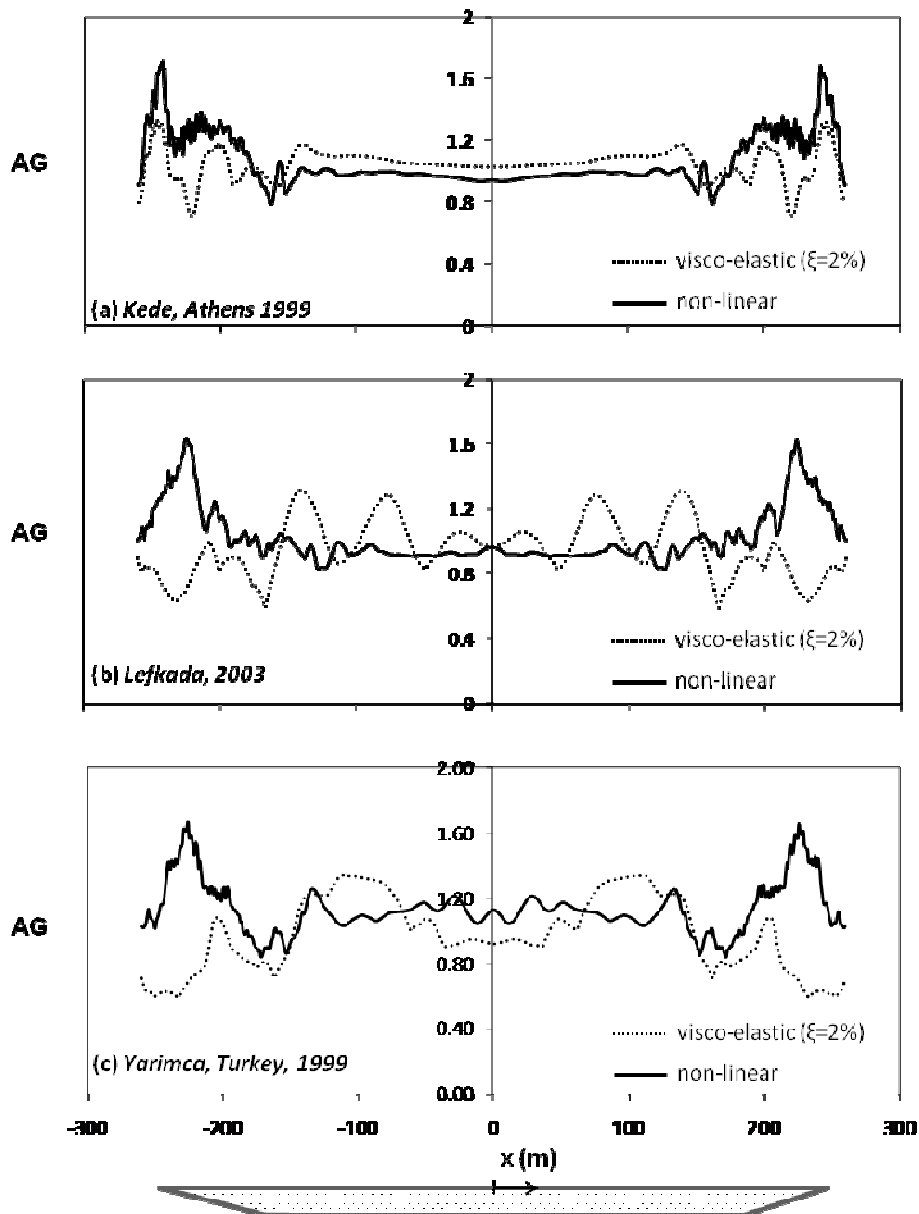


Figure 6: The effect of soil non-linearity – comparison of visco-elastic with nonlinear (with the kinematic hardening constitutive model) analyses using real records as seismic excitation. Distributions of the aggravation factor AG along the valley surface for : (a) the Kede, Athens 1999 record; (b) the Lefkada 2003 record; and (c) the Yarimca, Kocaeli 1999 record

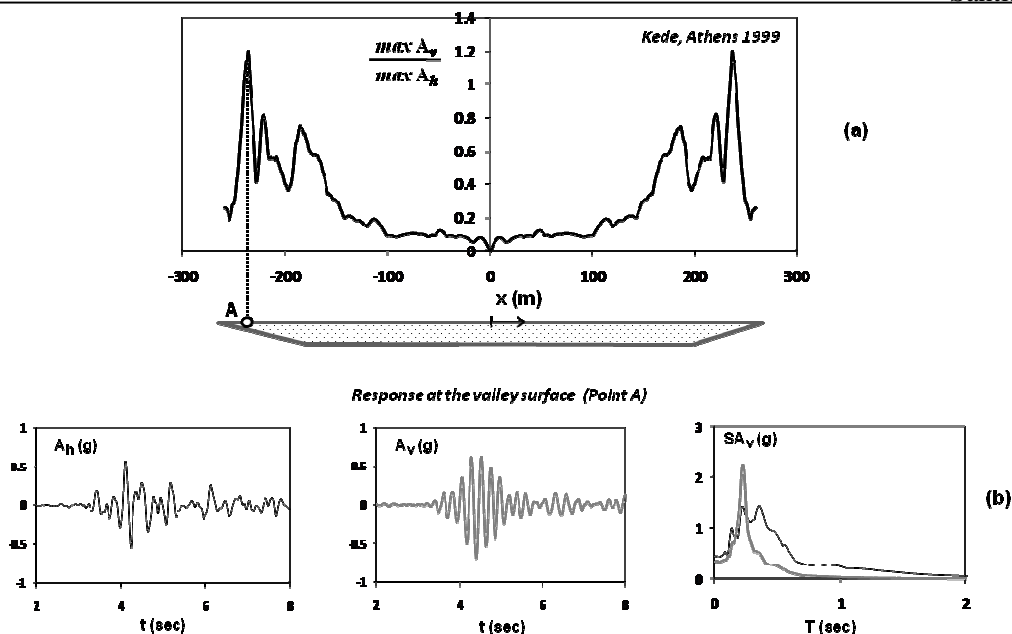


Figure 7 : Generation of “parasitic” vertical component – elastic analysis ($\xi = 2\%$) using the *horizontal* component of the Kede, Athens 1999 record as the sole seismic excitation; (a) distribution of the ratio of vertical to horizontal acceleration component along the valley surface and (b) horizontal and vertical acceleration time histories at the point A of the valley surface and elastic response of horizontal (black line) and vertical (gray line) acceleration at the same point

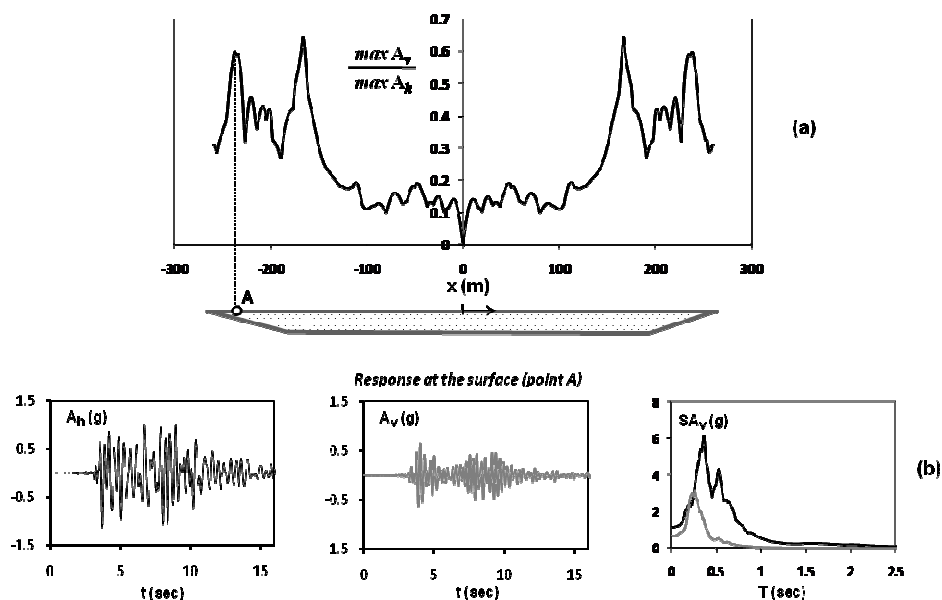


Figure 8 : Generation of “parasitic” vertical component – elastic analysis ($\xi = 2\%$) using the *horizontal* component of the Lefkada, 2003 record as the sole seismic excitation; (a) distribution of the ratio of vertical to horizontal acceleration component along the valley surface and (b) horizontal and vertical acceleration time histories at the point A of the valley surface and elastic response of both the horizontal (black line) and vertical (grey line) acceleration at the same point

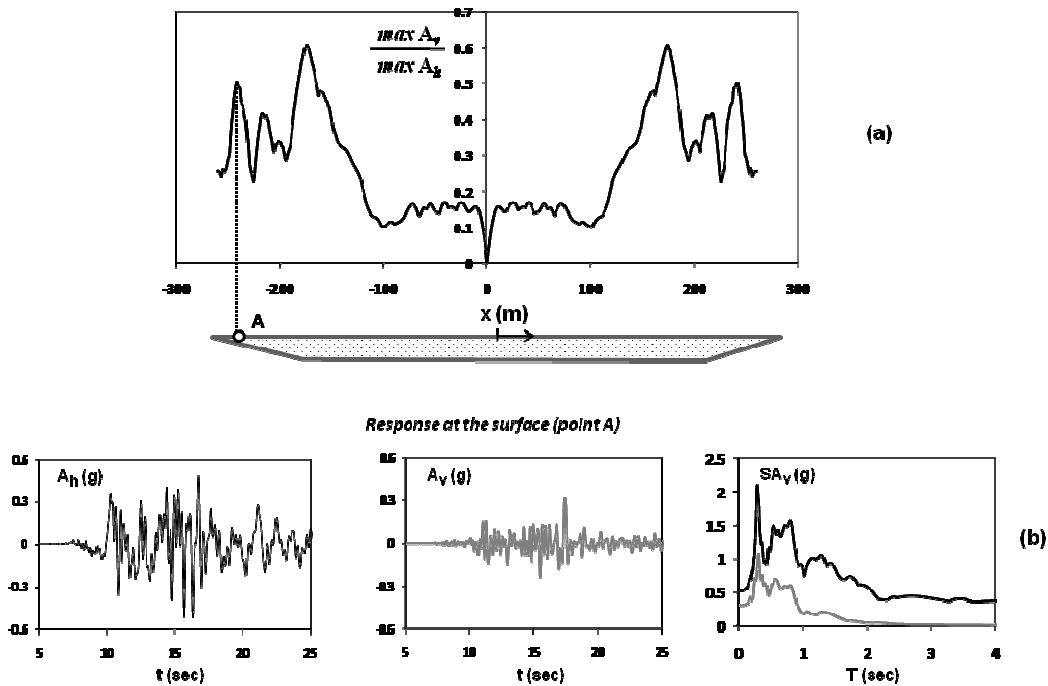


Figure 9 : Generation of “parasitic” vertical component – elastic analysis ($\xi = 2\%$) using the *horizontal* component of the Yarimca, 1999 record as the sole seismic excitation; (a) distribution of the ratio of vertical to horizontal acceleration component along the valley surface and (b) horizontal and vertical acceleration time histories at the point A of the valley surface and elastic response of both the horizontal (black line) and vertical (grey line) acceleration at the point A of the valley surface

ACKNOWLEDGEMENTS

This work was partially supported by the EU 7th Framework research project funded through the European Research Council’s Programme “Ideas”, Support for Frontier Research – Advanced Grant. Contract number ERC-2008-AdG 228254-DARE

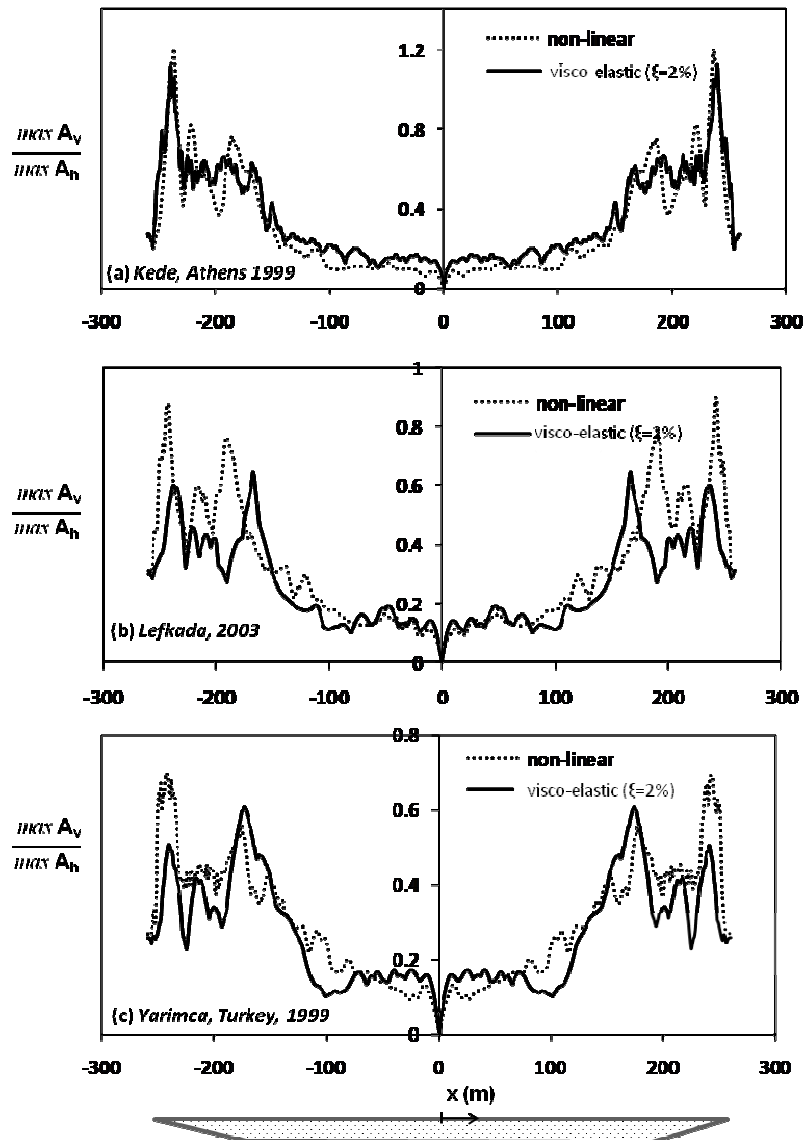


Figure 10: The effect of soil-nonlinearity on the parasitic vertical component of motion. Comparison of viscoelastic with nonlinear analysis using only horizontal components of real records as seismic excitation. Distributions of the ratio of vertical to horizontal acceleration along the valley surface for : (a) the Kede, Athens 1999 record; (b) the Lefkada 2003 record; and (c) the Yarımcı, Turkey, 1999 record.

REFERENCES

- ABAQUS, Inc. (2008), *ABAQUS user's manual*, Providence, R.I.
- Anastasopoulos I., Gelagoti F., Kourkoulis R., and Gazetas G. (2010). "Simplified Constitutive Model for Simulation of Cyclic Response of Surface Foundations: Validation against Laboratory Tests", *Journal of Geotechnical and Geoenvironmental Engineering*, (accepted for publication).

5th International Conference on Earthquake Geotechnical Engineering

January 2011, 10-13

Santiago, Chile

-
- Bao H., Bielak J., Ghattas O., Kallivokas L.F., O' Hallaron D.R., Shewchuk J., & Xu J. (1996). Earthquake ground motion modeling on parallel computers. *Proceedings of ACM/IEEE Supercomputing Conference*, Pittsburgh, USA.
- Bard P.Y. & Bouchon M.A. (1980). The seismic response of sediment filled valleys, Parts I-II. *BSSA*, Vol.70.
- Bielak J., Xu J., & Ghattas O. (1999). Earthquake Ground motion and Structural Response in alluvial Valleys. *Journal of Geotechnical and Geoenvironmental Engineering*, May 1999.
- Bielak J., Hisada Y., Bao H., Xu J. & Ghattas O. (2000). One - vs two - or three-dimensional effects in sedimentary valleys. *Proceedings of the 12th World Conference on Earthquake Engineering*, New Zealand.
- Bouchon M. (1973). Effect of topography on surface motion. *BSSA*, Vol.63, pp.615-632.
- Fishman K. L. and Ahmad S. (1995). Seismic response for alluvial valleys subjected to SH, P and SV waves. *Soil Dynamics and Earthquake Engineering*, 14, pp. 249-258.
- Gelagoti F., Gazetas G., Kourkoulis R. (2007) "2D Valley Effects : How predictable and important are they?", *Proceedings, 4th International Conference of Earthquake Geotechnical Engineering, Thessaloniki, 2007*
- Harmsen, S. C., and S. T. Harding (1981). Surface motion over a sedimentary valley for incident plane P and SV waves, *BSSA*, 72, 655-670.
- Ishibashi I., Zhang X. (1993), Unified dynamic shear moduli and damping ratios of sand and clay, *Soils and Foundations*, 33(1), pp. 182-191.
- Kawase H. (1987). Time-domain response of a semicircular canyon for incident SV, P, and Rayleigh waves calculated by the discrete wave number boundary element method, *BSSA*,
- Ohtsuki A. & Harumi K. (1983). Effect of topography and subsurface inhomogeneities on seismic SV waves. *Journal of Earthquake Engineering & Structural Dynamics*, Vol. 11, pp. 441-462.
- Sanchez-Sesma, F. J., and E. Rosenblueth (1979), Ground motions at canyons of arbitrary shape under incident plane SH waves. *Int. Journal of Earthquake Engineering and Structural Dynamics*, 7, pp. 441-450.
- Tazoh T., Dewa K., Shimizu K., & Shimada M. (1984), Observations of earthquake response behavior of foundation piles for road bridge, *Proceedings of the 8th World Conference on Earthquake Engineering*, 3, pp. 577-584.
- Trifunac M.D. (1971), Surface motion of a semi-cylindrical alluvial valley for incident plane SH waves. *BSSA*, Vol.61, pp.1755-1770.
- Trifunac M.D. (1973), Scattering of plane SH waves by a semi-cylindrical canyon, *Earthquake Engineering and Structural Dynamics*, Vol. 1, pp. 267-281.
- Zhang B. and Papageorgiou A. (1996). Simulation of the Response of the Marina District Basin, San Francisco, California, to the 1989 Loma Prieta Earthquake. *BSSA*, Vol. 86, No. 5, pp. 1382-1400.